PHYSICAL REVIEW D **81,** 016012 (2010)

Analysis of the $B_c \to D_1^0 l\nu$ decay

N. Ghahramany* and R. Khosravi†

Physics Department, Shiraz University, Shiraz 71454, Iran

(Received 18 April 2009; published 22 January 2010)

The structure of the $D_1^0(2420[2430])$, $(J^P = 1^+)$ mesons via analyzing the semileptonic $B_c \to D_1^0 l\nu$ transition is considered in the framework of the three-point QCD sum rules. In this work, we consider the $D_1^0(2420[2430])$ axial vectors as conventional $c\bar{u}$ mesons. Taking into account the gluon condensate contributions, the relevant form factors are obtained. The obtained results for the form factors are used to evaluate the decay rate and the branching ratio.

DOI: 10.1103/PhysRevD.81.016012 PACS numbers: 11.55.Hx, 12.39.Hg, 13.20.He

I. INTRODUCTION

The structure of the even-parity charmed mesons ($J^P = 1^+$) is not known exactly yet and has been debated in the quark model. There is some difference between the measured and predicted masses of them, observed in the laboratories [1–5] and considered in many phenomenological models [6–11]. Much effort has been dedicated to realize this unexpected disparity between theory and experiment. Therefore the study of the processes involving these mesons is important for understanding the structure and quark content of them. Some physicists presume that these discovered states are conventional $c\bar{u}$ and $c\bar{s}$ mesons [12–20]. Among these mesons, we focus on the nonstrange D_1^0 meson. So far the two confirmed D_1^0 states, with masses of 2423.4 ± 3.2 MeV and $2427 \pm 26 \pm 25$ MeV, have been observed [5]. The narrow-width state with lower mass is known as $D_1^0(2420)$ and the wide-width state with more mass is identified as $D_1^0(2430)$ [21]. In this work, we plan to analyze the $D_1^0(2420[2430])$ axial vectors as conventional mesons with a $|c\bar{u}\rangle$ state.

The $B_c \to D^{*0} l\nu$ [22] and $B_c \to Dll/\nu\bar{\nu}$ [23] have been studied via three-point QCD sum rules (3PSR). The heavy meson B_c with $\bar{b}c$ quark structure is made of two heavy quarks with different charge and flavors. It is located between two heavy meson families, namely, charmonium $\bar{c}c$ and bottomonium $\bar{b}b$, so this meson is similar to the charmonium and bottomonium in the spectroscopy. The modern predictions for the mass spectra of $\bar{b}c$ levels were obtained in the potential models and lattice simulations [24–28]. But in contrast to charmonium and bottomonium, B_c decays only via weak interaction and possesses a long lifetime. For this reason the B_c transitions are a very interesting tool to calculate more precise values for the Cabibbo-Kabayashi-Maskawa (CKM) matrix elements and to study the CP and T violations that occur in weak interactions.

In this work, we analyze the semileptonic $B_c \to D_1^0(2420[2430])l\nu$ decays in the 3PSR. To this aim, taking into account the gluon condensate corrections as the important term of the nonperturbative part of the correlation function, the form factors of the $B_c \to D_1^0$ transition are obtained within the 3PSR. The form factors of the $B_c \to D_1^0(2420[2430])$ transitions are a function of the transferred momentum square q^2. So, we plot these form factors and the differential decay branching fraction of these decays with respect to q^2. Also the branching ratios for these cases are evaluated. Detection of these channels and their comparison with the phenomenological models like QCD sum rules could give useful information about the structure of the D_1^0 meson.

This paper is organized as follow. In Sec. II, we calculate the form factors for the $B_c \to D_1^0$ transition in the 3PSR. Finally, Sec. III is devoted to the numeric results and discussions.

II. SUM RULES METHOD

In this section, we study the transition form factors of the semileptonic $B_c \to D_1^0 l\nu$ decay by the QCD sum rules mechanism. To this aim, we consider the D_1^0 meson as the $|c\bar{u}\rangle$ state. The $B_c \to D_1^0 l\nu$ process is governed by the tree level $b \to ul\nu$ transition and the c quark is the spectator, at quark level (see Fig. 1). The three-point correlation function is considered for the evaluation of the transition form factors in the framework of the 3PSR. The three-point correlation function is constructed from the vacuum expectation value of the time ordered product of three currents as follows:

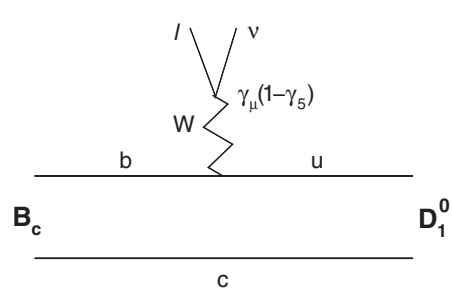

FIG. 1. The bare-loop diagram for the $B_c \to D_1^0 l\nu$ transition.

*ghahramany@susc.ac.ir
†khosravi.reza@gmail.com

$$\Pi_{\mu\nu}(p^2, p'^2, q^2) = i^2 \int d^4x d^4y e^{+ip'x-ipy} \times \langle 0|T\{J_\nu^{D_1^0}(x) J_\mu^W(0) J^{B_c\dagger}(y)\}|0\rangle, \quad (1)$$

where $q^2 = (p - p')^2$, and p and p' are the momentum of the initial and final meson states, respectively. $J_\nu^{D_1^0}(x) = \bar{c}\gamma_\nu\gamma_5 u$ and $J^{B_c}(y) = \bar{c}\gamma_5 b$ are the interpolating currents of the D_1^0 and B_c mesons. $J_\mu^W = \bar{u}\gamma_\mu(1-\gamma_5)b$ is the current of the weak transition.

We can obtain the correlation function of Eq. (1) in two parts. The phenomenological or physical part is calculated saturating the correlation by a tower of hadrons with the same quantum numbers as interpolating currents. The QCD or theoretical part, on the other sidem is obtained in terms of the quarks and gluons interacting in the QCD vacuum. To derive the phenomenological part of the correlation given in Eq. (1), two complete sets of intermediate states with the same quantum numbers as the currents $J_{D_1^0}$ and J_{B_c} are inserted. This procedure leads to the following representation of the above-mentioned correlation:

$$\Pi_{\mu\nu}(p^2, p'^2, q^2) = \frac{\langle 0 \mid J_\nu^{D_1^0} \mid D_1^0(p', \varepsilon)\rangle\langle D_1^0(p', \varepsilon) \mid J_\mu^W \mid B_c(p)\rangle\langle B_c(p) \mid J^{B_c\dagger} \mid 0\rangle}{(p'^2 - m_{D_1^0}^2)(p^2 - m_{B_c}^2)} + \text{higher resonances and continuum states.} \quad (2)$$

The general expression for the hadronic matrix element of the weak current with definition of the transition form factors is given by the formula:

$$\langle D_1^0(p', \varepsilon) \mid \bar{u}\gamma_\mu(1-\gamma_5)b \mid B_c(p)\rangle = f_V'(q^2)\varepsilon_{\mu\nu\alpha\beta}\varepsilon^{*\nu}p^\alpha p'^\beta - i[f_0'(q^2)\varepsilon_\mu^* + f_1'(q^2)(\varepsilon^* p)P_\mu + f_2'(q^2)(\varepsilon^* p)q_\mu], \quad (3)$$

where

$$\begin{aligned} f_V'(q^2) &= \frac{2f_V(q^2)}{(m_{B_c} + m_{D_1^0})}, \\ f_0'(q^2) &= f_0(q^2)(m_{B_c} + m_{D_1^0}), \\ f_1'(q^2) &= -\frac{f_1(q^2)}{(m_{B_c} + m_{D_1^0})}, \\ f_2'(q^2) &= -\frac{f_2(q^2)}{(m_{B_c} + m_{D_1^0})}, \end{aligned} \quad (4)$$

and the $f_V(q^2)$, $f_0(q^2)$, $f_1(q^2)$, and $f_2(q^2)$ are the transition form factors, $P_\mu = (p + p')_\mu$, $q_\mu = (p - p')_\mu$, and ε is the four-polarization vector of the D_1^0 meson. Also the following matrix elements are defined in the standard way in terms of the leptonic decay constants of the D_1^0 and B_c mesons as

$$\begin{aligned} \langle 0 \mid J_{D_1^0}^\nu \mid D_1^0(p', \varepsilon)\rangle &= f_{D_1^0} m_{D_1^0} \varepsilon^\nu, \\ \langle 0 \mid J_{B_c} \mid B_c(p)\rangle &= i\frac{f_{B_c} m_{B_c}^2}{m_b + m_c}, \end{aligned} \quad (5)$$

where $f_{D_1^0}$ and f_{B_c} are the leptonic decay constants of D_1^0 and B_c mesons, respectively. Using Eqs. (3) and (5) in Eq. (2) and performing a summation over the polarization of the D_1^0 meson, we get the following result for the physical part:

$$\Pi_{\mu\nu}(p^2, p'^2, q^2) = -\frac{f_{B_c} m_{B_c}^2}{(m_b + m_c)} \frac{f_{D_1^0} m_{D_1^0}}{(p'^2 - m_{D_1^0}^2)(p^2 - m_{B_c}^2)} \times [i f_V'(q^2)\varepsilon_{\mu\nu\alpha\beta}p^\alpha p'^\beta + f_0'(q^2)g_{\mu\nu} + f_1'(q^2)P_\mu p_\nu + f_2'(q^2)q_\mu p_\nu] + \text{excited states.} \quad (6)$$

The coefficients of Lorentz structures $i\epsilon_{\mu\nu\alpha\beta}p^\alpha p'^\beta$, $g_{\mu\nu}$, $P_\mu p_\nu$, and $q_\mu p_\nu$ in the correlation function $\Pi_{\mu\nu}$ will be chosen in determination of the form factors $f_V(q^2)$, $f_0(q^2)$, $f_1(q^2)$, and $f_2(q^2)$, respectively. So the Lorentz structures in the correlation function can be written down as

$$\Pi_{\mu\nu}(p^2, p'^2, q^2) = i\Pi_V\varepsilon_{\mu\nu\alpha\beta}p^\alpha p'^\beta + \Pi_0 g_{\mu\nu} + \Pi_1 P_\mu p_\nu + \Pi_2 q_\mu p_\nu, \quad (7)$$

where each Π_i function is defined in terms of the perturbative and nonperturbative parts as

$$\Pi_i(p^2, p'^2, q^2) = \Pi_i^{\text{per}}(p^2, p'^2, q^2) + \Pi_i^{\text{nonper}}(p^2, p'^2, q^2). \quad (8)$$

With the help of the operator product expansion (OPE), in the deep Euclidean region where $p^2 \ll (m_b + m_c)^2$ and $p'^2 \ll m_c^2$, the vacuum expectation value of the expansion of the correlation function in terms of the local operators, is written as follows [22,29]:

$$\Pi_{\mu\nu}(p^2, p'^2, q^2) = (C_0)_{\mu\nu} + (C_3)_{\mu\nu}\langle\bar{q}q\rangle + (C_4)_{\mu\nu} \times \langle G_{\alpha\beta}^a G^{a\alpha\beta}\rangle + (C_5)_{\mu\nu} \times \langle\bar{q}\sigma_{\alpha\beta}T^a G^{a\alpha\beta}q\rangle + (C_6)_{\mu\nu} \times \langle\bar{q}\Gamma q\bar{q}\Gamma' q\rangle + \cdots, \quad (9)$$

where $(C_i)_{\mu\nu}$ are the Wilson coefficients, $G_{\alpha\beta}^a$ is the gluon field strength tensor, and Γ and Γ' are the matrices appearing in the calculations. The nonperturbative part contains

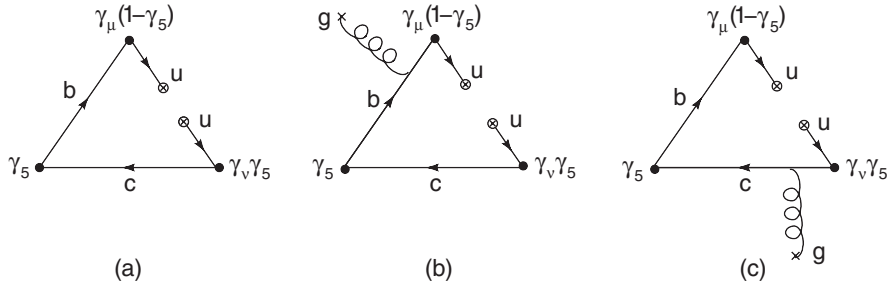

FIG. 2. Contribution of condensates with mass dimensions 3 and 5. The quark-quark condensate and quark-gluon condensate are shown in (a) and (b), (c) for the $B_c \to D_1^0$ transition, respectively.

the quark and gluon condensate diagrams. We consider the condensate terms of dimension 3, 4, and 5. It is found that the heavy quark condensate contributions are suppressed by the inverse of the heavy quark mass and can be safely omitted. So there are three diagrams with mass dimensions 3 and 5. These diagrams are shown in Fig. 2. Let us consider the condensate contribution of the quark-quark. After some calculations for Fig. 2(a), we have

$$(C_3)_{\mu\nu} = -\frac{1}{4}\,\mathrm{Tr}[F(p,k)] + \frac{m_u}{16} \times \mathrm{Tr}\Bigg[\left(\frac{\partial}{\partial p^\alpha} + \frac{\partial}{\partial k^\alpha}\right) \times F(p,k)\gamma_\alpha\Bigg] + \frac{1}{32}\left(m_u^2 - \frac{m_0^2}{2}\right) \times \mathrm{Tr}\Bigg[\left(\frac{\partial^2}{\partial p^\alpha \partial k^\alpha} + \frac{\partial^2}{(\partial p^\alpha)^2} + \frac{\partial^2}{(\partial k^\alpha)^2}\right)F(p,k)\Bigg], \tag{10}$$

where $m_0^2 = 0.8 \pm 0.2\ \mathrm{GeV}^2$ and $F(p,k)$ is

$$F(p,k) = \left(\gamma_\mu(1-\gamma_5)\frac{i}{(\not p + \not k) - m_b}\gamma_5 \frac{i}{\not k - m_c}\gamma_\nu\gamma_5\right),$$

where k is the momentum of the c quark. The contribution of this diagram is zero after applying the double Borel transformation with respect to both variables p^2 and p'^2, because only one variable appears in the denominator. In similar way, it can be shown that the condensate contributions of other diagrams are zero after applying the double Borel transformation.

In the QCD sum rule method, the OPE is truncated at some finite order such that Borel transformations play an important role in this cutting. Usually, the proper regions of the Borel parameters are adopted by demanding that in the truncated OPE, the condensate term with the highest dimension remains a small fraction of the sum of all terms. These regions keep the convergence of the condensate expansion under control and guarantee that one does not introduce a large error neglecting the higher-dimensional terms. In the numerical analysis section, we explain how these proper regions are obtained. So we will not consider the condensates with $d \geq 6$ that play a minor role in our calculations.

Therefore in this case, we consider the two gluon condensate diagrams with mass dimension 4 as a important term of the nonperturbative corrections only, i.e.,

$$\Pi_i(p^2, p'^2, q^2) = \Pi_i^{\mathrm{per}}(p^2, p'^2, q^2) + \Pi_i^{\langle G^2\rangle}(p^2, p'^2, q^2) \times \left\langle \frac{\alpha_s}{\pi} G^2 \right\rangle. \tag{11}$$

The diagrams for the contribution of the gluon condensates are depicted in Fig. 3.

Using the double dispersion representation, the bare-loop contribution is determined

$$\Pi_i^{\mathrm{per}} = -\frac{1}{(2\pi)^2}\iint \frac{\rho_i^{\mathrm{per}}(s,s',q^2)}{(s-p^2)(s'-p'^2)}\,ds\,ds' + \text{subtraction terms}. \tag{12}$$

By replacing the propagators with the Dirac-delta functions (Cutkosky rules):

$$\frac{1}{k^2 - m^2} \to -2i\pi\delta(k^2 - m^2), \tag{13}$$

the spectral densities $\rho_i^{\mathrm{per}}(s,s',q^2)$ are found as

$$\begin{aligned}
\rho_V^{\mathrm{per}} &= 4N_c I_0(s,s',q^2)\{B_1(m_b - m_c) - B_2(m_u + m_c) - m_c\},\\
\rho_0^{\mathrm{per}} &= -2N_c I_0(s,s',q^2)\{\Delta(m_c + m_u) - \Delta'(m_b - m_c) - 4A_1(m_b - m_c) + 2m_c^2(m_b - m_c - m_u) + m_c(2m_b m_u - u)\},\\
\rho_1^{\mathrm{per}} &= 2N_c I_0(s,s',q^2)\{B_1(m_b - 3m_c) - B_2(m_c + m_u) + 2A_2(m_b - m_c) + 2A_3(m_b - m_c) - m_c\},\\
\rho_2^{\mathrm{per}} &= 2N_c I_0(s,s',q^2)\{2A_2(m_b - m_c) - 2A_3(m_b - m_c) - B_1(m_b + m_c) + B_2(m_c + m_u) + m_c\},
\end{aligned} \tag{14}$$

where

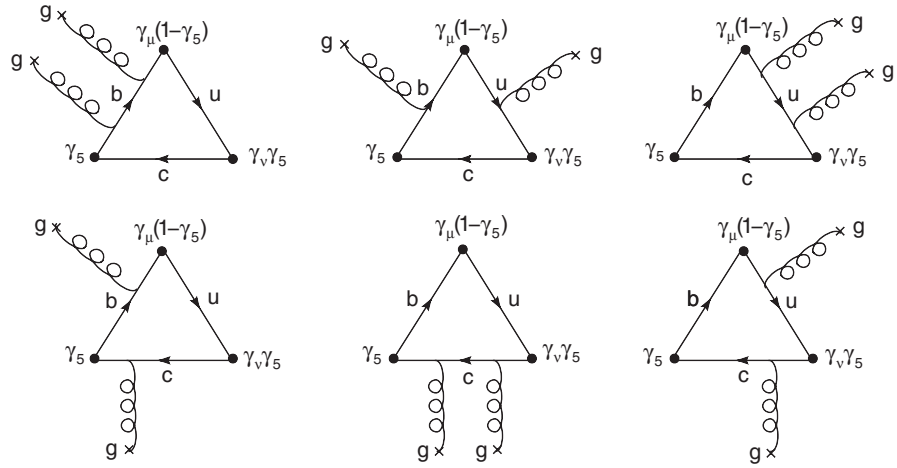

FIG. 3. Contribution of two gluon condensates with mass dimension 4 for the $B_c \to D_1^0$ transition.

$$I_0(s, s', q^2) = \frac{1}{4\lambda^{1/2}(s, s', q^2)}, \qquad B_1 = \frac{1}{\lambda(s, s', q^2)}[2s'\Delta - \Delta' u], \qquad B_2 = \frac{1}{\lambda(s, s', q^2)}[2s\Delta' - \Delta u],$$

$$A_1 = -\frac{1}{2\lambda(s, s', q^2)}[(4ss'm_c^2 - s\Delta'^2 - s'\Delta^2 - u^2 m_c^2 + u\Delta\Delta')],$$

$$A_2 = -\frac{1}{\lambda^2(s, s', q^2)}[8ss'^2 m_c^2 - 2ss'\Delta'^2 - 6s'^2\Delta^2 - 2u^2 s' m_c^2 + 6s'u\Delta\Delta' - u^2\Delta'^2],$$

$$A_3 = \frac{1}{\lambda^2(s, s', q^2)}[4ss'um_c^2 + 4ss'\Delta\Delta' - 3su\Delta'^2 - 3u\Delta^2 s' - u^3 m_c^2 + 2u^2\Delta\Delta'],$$

and $N_c = 3$ is the color factor. Also $\lambda(a, b, c) = a^2 + b^2 + c^2 - 2ac - 2bc - 2ab$, $u = s + s' - q^2$, $\Delta = s + m_c^2 - m_b^2$, and $\Delta' = s' + m_c^2 - m_u^2$.

To obtain the contributions of the gluon condensate diagrams (Fig. 3), the Fock-Schwinger fixed-point gauge $x^\mu A_\mu^a = 0$ is used, where A_μ^a is the gluon field. In the evaluation of such diagrams in Fig. 3, integrals of the following types are encountered [30]:

$$\begin{aligned} I_0(a, b, c) &= \int \frac{d^4k}{(2\pi)^4} \frac{1}{[k^2 - m_c^2]^a[(p+k)^2 - m_b^2]^b[(p'+k)^2 - m_u^2]^c}, \\ I_\mu(a, b, c) &= \int \frac{d^4k}{(2\pi)^4} \frac{k_\mu}{[k^2 - m_c^2]^a[(p+k)^2 - m_b^2]^b[(p'+k)^2 - m_u^2]^c}, \\ I_{\mu\nu}(a, b, c) &= \int \frac{d^4k}{(2\pi)^4} \frac{k_\mu k_\nu}{[k^2 - m_c^2]^a[(p+k)^2 - m_b^2]^b[(p'+k)^2 - m_u^2]^c}. \end{aligned} \tag{15}$$

These integrals can be calculated using the Schwinger representation for the Euclidean propagator

$$\frac{1}{(k^2 + m^2)^n} = \frac{1}{\Gamma(\alpha)} \int_0^\infty d\alpha \alpha^{n-1} e^{-\alpha(k^2+m^2)}. \tag{16}$$

After the Borel transformation, using

$$\mathcal{B}_{\hat{p}^2}(M^2) e^{-\alpha p^2} = \delta(1/M^2 - \alpha), \tag{17}$$

we obtain

$$\begin{aligned} \hat{I}_0(a, b, c) &= \frac{(-1)^{a+b+c}}{16\pi^2\Gamma(a)\Gamma(b)\Gamma(c)} (M_1^2)^{2-a-b}(M_2^2)^{2-a-c}\mathcal{U}_0(a+b+c-4, 1-c-b), \\ \hat{I}_\mu(a, b, c) &= \hat{I}_1(a, b, c)p_\mu + \hat{I}_2(a, b, c)p'_\mu, \\ \hat{I}_{\mu\nu}(a, b, c) &= \hat{I}_6(a, b, c)g_{\mu\nu} + \hat{I}_3(a, b, c)p_\mu p_\nu + \hat{I}_4(a, b, c)p_\mu p'_\nu + \hat{I}_4(a, b, c)p'_\mu p_\nu + \hat{I}_5(a, b, c)p'_\mu p'_\nu. \end{aligned} \tag{18}$$

$\hat{I}$ in Eq. (18) stands for the double Borel transformed form of Eq. (15), in Schwinger representation, where

$$\begin{aligned}
\hat{I}_k(a,b,c) &= i\frac{(-1)^{a+b+c+1}}{16\pi^2\Gamma(a)\Gamma(b)\Gamma(c)}(M_1^2)^{1-a-b+k}(M_2^2)^{4-a-c-k}\mathcal{U}_0(a+b+c-5,1-c-b),\\
\hat{I}_m(a,b,c) &= i\frac{(-1)^{a+b+c+1}}{16\pi^2\Gamma(a)\Gamma(b)\Gamma(c)}(M_1^2)^{-a-b-1+m}(M_2^2)^{7-a-c-m}\mathcal{U}_0(a+b+c-5,1-c-b),\\
\hat{I}_6(a,b,c) &= i\frac{(-1)^{a+b+c+1}}{32\pi^2\Gamma(a)\Gamma(b)\Gamma(c)}(M_1^2)^{3-a-b}(M_2^2)^{3-a-c}\mathcal{U}_0(a+b+c-6,2-c-b),
\end{aligned} \tag{19}$$

where $k = 1, 2$, $m = 3, 4, 5$, M_1^2 and M_2^2 are the Borel parameters in the s and s' channels, respectively, and the function $\mathcal{U}_0(a,b)$ is defined as

$$\mathcal{U}_0(a,b) = \int_0^\infty dy(y+M_1^2+M_2^2)^a y^b \times \exp\left[-\frac{B_{-1}}{y} - B_0 - B_1 y\right],$$

where

$$\begin{aligned}
B_{-1} &= \frac{1}{M_1^2M_2^2}[m_u^2M_1^4 + m_b^2M_2^4 + M_2^2M_1^2(m_b^2+m_u^2-q^2)],\\
B_0 &= \frac{1}{M_1^2M_2^2}[(m_u^2+m_c^2)M_1^2 + M_2^2(m_b^2+m_c^2)],\\
B_1 &= \frac{m_c^2}{M_1^2M_2^2}.
\end{aligned} \tag{20}$$

By performing the double Borel transformations over the variables p^2 and p'^2 on the physical parts of the correlation function and bare-loop diagrams and also equating two representations of the correlation function, the sum rules for the $f_i'(q^2)$ are obtained:

$$\begin{aligned}
f_i'(q^2) = &-\frac{(m_b+m_c)}{f_{B_c}m_{B_c}^2 f_{D_1^0}m_{D_1^0}} e^{m_{B_c}^2/M_1^2} e^{m_{D_1}^2/M_2^2}\\
&\times\left\{-\frac{1}{4\pi^2}\int_{m_c^2+m_u^2}^{s_0'} ds' \int_{s_L}^{s_0} \rho_i^{\rm per}(s,s',q^2)\right.\\
&\left.\times e^{-s/M_1^2}e^{-s'/M_2^2} - iM_1^2M_2^2\left\langle\frac{\alpha_s}{\pi}G^2\right\rangle\frac{C_i^4}{6}\right\},
\end{aligned} \tag{21}$$

where $i = V$, 0, 1, and 2, s_0 and s_0' are the continuum thresholds in pseudoscalar B_c and axial vector D_1^0 channels, respectively, and the lower bound integration limit s_L is

$$s_L = \frac{(m_c^2+q^2-m_b^2-s')(m_b^2s'-m_c^2q^2)}{(m_b^2-q^2)(m_c^2-s')}.$$

The explicit expressions for C_i^4 are presented in the Appendix.

III. NUMERICAL ANALYSIS

Now, we present our numerical analysis of the form factors $f_i(q^2)$ ($i = V$, 0, 1, 2) via the 3PSR. From the sum rule expressions of the form factors, it is clear that the main input parameters entering the expressions are gluon condensates, an element of the CKM matrix V_{ub}, leptonic decay constants f_{B_c} and $f_{D_1^0}$, Borel parameters M_1^2 and M_2^2, as well as the continuum thresholds s_0 and s_0'. We choose the values of the gluon condensate, leptonic decay constants, CKM matrix element, quark and meson masses as $\langle\frac{\alpha_s}{\pi}G^2\rangle = (0.009 \pm 0.007)$ GeV^4 [31], $f_{D_1^0} = (225 \pm 25)$ MeV, $f_{B_c} = (350 \pm 25)$ MeV [32], $|V_{ub}| = (0.004\,31 \pm 0.000\,30)$, $m_u = (1.5$–$3.3)$ MeV, $m_c = (1270^{+70}_{-110})$ MeV, $m_b = (4200^{+170}_{-70})$ MeV, $m_{D_1^0(2420)} = (2423.4 \pm 3.2)$ MeV, $m_{D_1^0(2430)} = (2427 \pm 26 \pm 25)$ MeV, and $m_{B_c} = (6276 \pm 4)$ MeV [21].

The sum rules for the form factors also contain four auxiliary parameters: Borel mass squares M_1^2 and M_2^2 and continuum thresholds s_0 and s_0'. These are not physical quantities, so the form factors as physical quantities should be independent of them. The parameters s_0 and s_0', which are the continuum thresholds of B_c and D_1^0 mesons, respectively, are determined from the condition that guarantees the sum rules to practically be stable in the allowed regions for M_1^2 and M_2^2. The values of the continuum thresholds calculated from the two-point QCD sum rules are taken to be $s_0 = (45$–$50)$ GeV^2 and $s_0' = (6$–$8)$ GeV^2 [33–35]. The working regions for M_1^2 and M_2^2 are determined requiring that not only the contributions of the higher states and continuum are small, but the contributions of the operators with higher dimensions are also small. Both conditions are satisfied in the regions $10\ \text{GeV}^2 \le M_1^2 \le 25\ \text{GeV}^2$ and $8\ \text{GeV}^2 \le M_2^2 \le 15\ \text{GeV}^2$. The dependence of the form factors on M_1^2 and M_2^2 for the $B_c \to D_1^0(2420[2430])l\nu$ decays is shown in Fig. 4. This figure shows a good stability of the form factors with respect to the Borel mass parameters in the working regions.

For analysis of the form factors of the semileptonic $B_c \to D_1^0(2420[2430])l\nu$ decays, we consider the $D_1^0(2420[2430])$ axial vectors as conventional mesons, i.e., the $|c\bar{u}\rangle$ state. Using Eqs. (4) and (21), the values of the form factors at $q^2 = 0$ are presented in Table I. It should be remarked that, the values of the transition form factors at $q^2 = 0$ for $B_c \to D_1^0(2420)l\nu$ decay are the same as those for the $B_c \to D_1^0(2430)l\nu$. Our calculations show

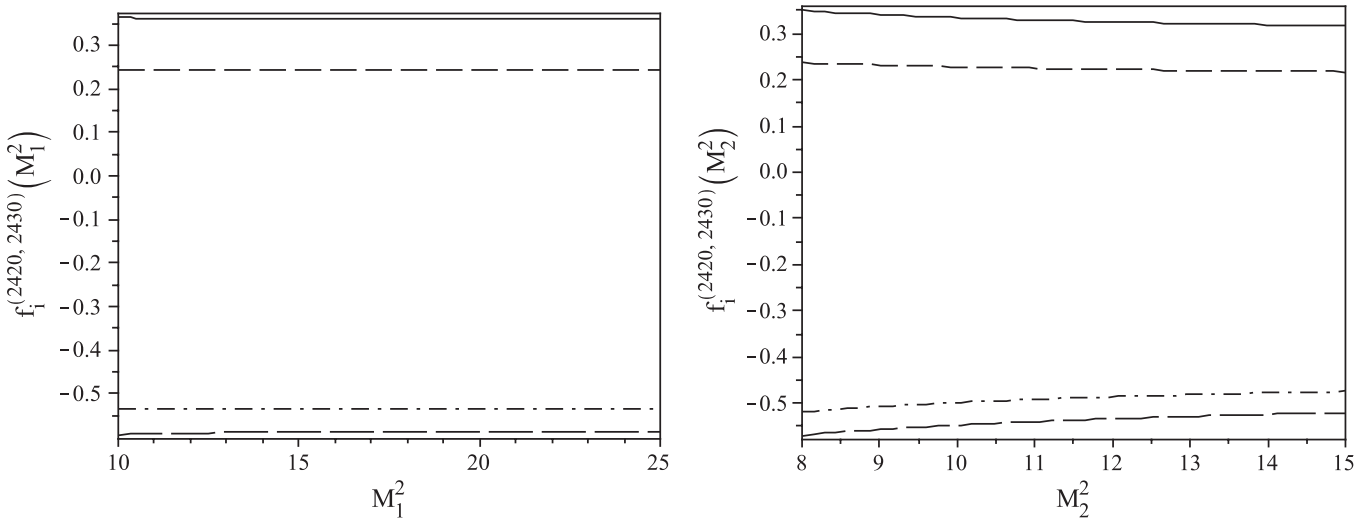

FIG. 4. The dependence of the $f_i^{(2420,2430)}$ form factors on M_1^2 and M_2^2. The solid, dashed, dash-dotted, and long-dashed lines correspond to f_1, f_0, f_V, and f_2, respectively.

the other physical quantities of these decays are nearly the same.

The sum rules for the form factors are truncated at about 9 GeV^2, so to extend our results to the full physical region, we look for a parametrization of the form factors in such a way that in the region $0 \leq q^2 \leq (m_{B_c} - m_{D_1^0})^2$ GeV^2, this parametrization coincides with the sum rule predictions. Our numerical calculations show that the sufficient parametrization of the form factors with respect to q^2 is

$$f_i(q^2) = \frac{a}{(1 - \frac{q^2}{m_{\rm fit}^2})} + \frac{b}{(1 - \frac{q^2}{m_{\rm fit}^2})^2}. \tag{22}$$

The values of the parameters a, b, and $m_{\rm fit}$ are given in Table II. Figure 5 depicts the fit functions of the $f_i^{(2420,2430)}(q^2)$ ($i = V$, 0, 1, 2) form factors for the $B_c \to D_1^0(2420[2430])l\nu$ decays with respect to the transferred momentum square q^2. This figure also contains the form factors obtained via the 3PSR [see Eq. (21)]. The form factors and their fit functions coincide well in the interval $0 \leq q^2 \leq 9$ GeV^2.

In order to parametrize each form factor to a fit function of Eq. (22), 50 data were entered. In other words, the values of $f_i(q^2)$ for 50 different values of q^2 were determined and then these determined values were fit to Eq. (22). If we want to find the errors in parameters a, b, and $m_{\rm fit}$ corresponding to the fit function, then we must consider the errors of 50 entered data which will be complicated due to the fit function structure. But since $f_i(0) = a + b$, and knowing that the error in $f_i(0)$ is about 25%–30% (see Table I), therefore the error in a and b is approximately 20%. The same amount of error is expected for $m_{\rm fit}$. We have considered this amount of error in the calculation of the $B_c \to D_1^0 l\nu$ branching ratio decay.

By using the expressions for the form factors, the differential decay width $d\Gamma/dq^2$ for the process $B_c \to D_1^0 l\nu$ ($l = e, \mu$) in terms of H_i is presented as follows:

$$\frac{d\Gamma_\pm(B_c \to D_1^0 l\nu)}{dq^2} = \frac{G_F^2|V_{ub}|^2}{192\pi^3 m_{B_c}^3} q^2 \lambda^{1/2}(m_{B_c}^2, m_{D_1^0}^2, q^2)|H_\pm|^2,$$
$$\frac{d\Gamma_0(B_c \to D_1^0 l\nu)}{dq^2} = \frac{G_F^2|V_{ub}|^2}{192\pi^3 m_{B_c}^3} q^2 \lambda^{1/2}(m_{B_c}^2, m_{D_1^0}^2, q^2)|H_0|^2,$$
$$\frac{d\Gamma_{\rm tot}(B_c \to D_1^0 l\nu)}{dq^2} = \frac{d\Gamma_\pm(B_c \to D_1^0 l\nu)}{dq^2} + \frac{d\Gamma_0(B_c \to D_1^0 l\nu)}{dq^2}, \tag{23}$$

where G_F is the Fermi constant, and $H_\pm$ and H_0 are defined

TABLE I. The value of the form factors for the $B_c \to D_1^0(2420[2430])$ transitions at $q^2 = 0$, $M_1^2 = 15$ GeV^2, and $M_2^2 = 10$ GeV^2.

$f_V^{(2420,2430)}(0)$	-0.53 ± 0.13
$f_0^{(2420,2430)}(0)$	0.24 ± 0.07
$f_1^{(2420,2430)}(0)$	0.35 ± 0.09
$f_2^{(2420,2430)}(0)$	-0.58 ± 0.15

TABLE II. Parameters appearing in the fit function for the form factors of the $B_c \to D_1^0(2420[2430])$ transitions at $M_1^2 = 15$ GeV^2 and $M_2^2 = 10$ GeV^2.

$f_i(q^2)$	a	b	$m_{\rm fit}$
$f_V^{(2420,2430)}(q^2)$	-0.35	-0.18	4.94
$f_0^{(2420,2430)}(q^2)$	0.20	0.04	6.88
$f_1^{(2420,2430)}(q^2)$	0.25	0.10	5.91
$f_2^{(2420,2430)}(q^2)$	-0.37	-0.21	4.82

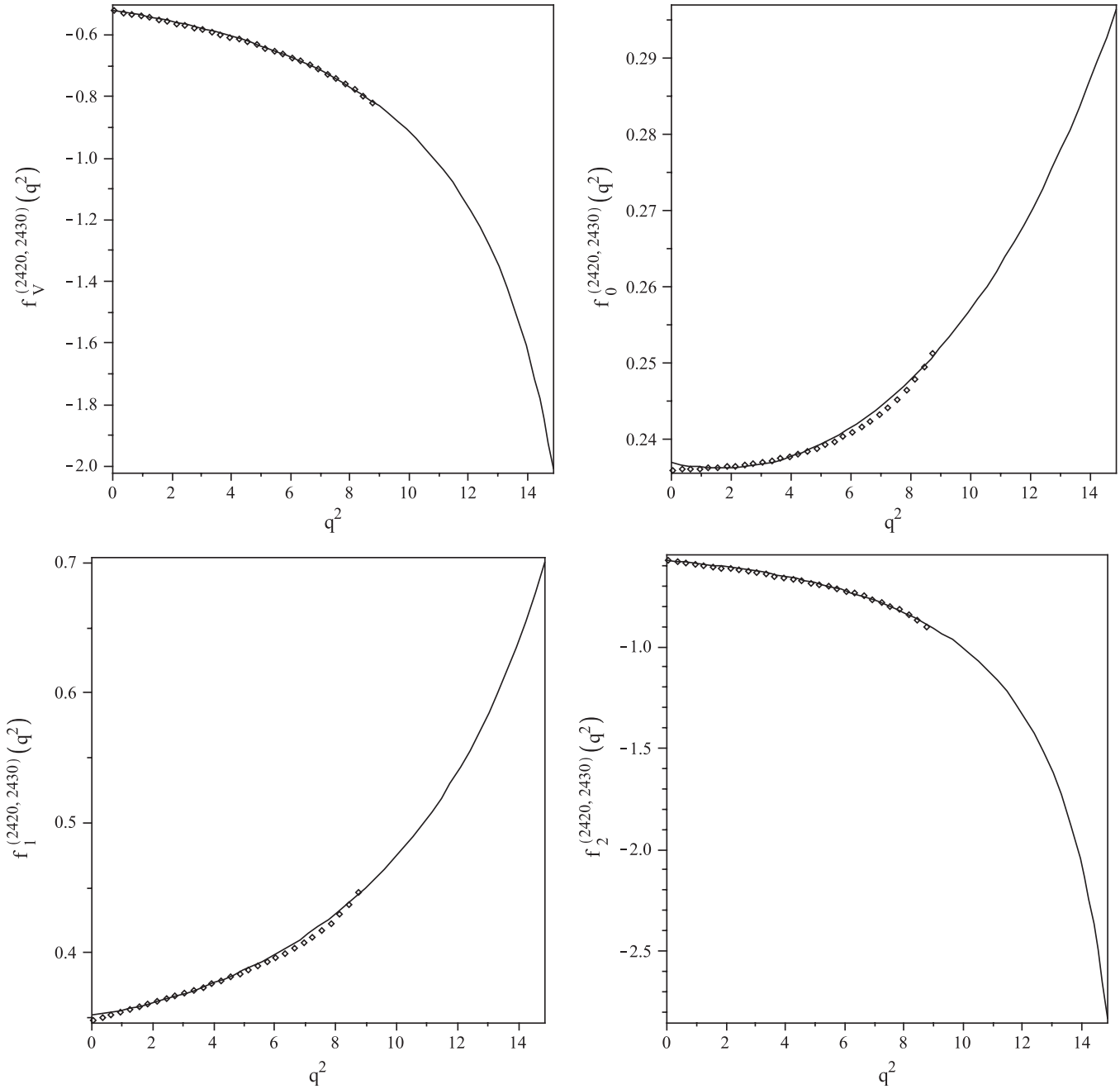

FIG. 5. The dependence of the form factors as well as the fit parametrization of the form factors on q^2. The squares correspond to the form factors, and the solid lines belong to the fit parametrization of the form factors.

as

$$H_\pm(q^2) = (m_{B_c} + m_{D_1^0}) f_0(q^2) \mp \frac{\lambda^{1/2}(m_{B_c}^2, m_{D_1^0}^2, q^2)}{m_{B_c} + m_{D_1^0}} f_V(q^2),$$

$$H_0(q^2) = \frac{1}{2m_{D_1^0}\sqrt{q^2}}\left[(m_{B_c}^2 - m_{D_1^0}^2 - q^2)(m_{B_c} + m_{D_1^0}) f_0(q^2) - \frac{\lambda(m_{B_c}^2, m_{D_1^0}^2, q^2)}{m_{B_c} + m_{D_1^0}} f_1(q^2)\right],$$

where $\pm$, 0 refer to the D_1^0 helicities. Note that in the limit of vanishing lepton mass (in our case electron and muon) the $f_2(q^2)$ form factor does not contribute to the decay width formula.

TABLE III. The branching ratio value of the semileptonic $B_c \to D_1^0(2420[2430])l\nu$ ($l = e, \mu$) decays within the 3PSR.

Mode	Br
$B_c \to D_1^0(2420[2430])l\nu$	$(3.89 \pm 1.21) \times 10^{-5}$

To calculate the branching ratios of the $B_c \to D_1^0(2420[2430])l\nu$ ($l = e, \mu$) decays, we integrate Eq. (23) over q^2 in the whole physical region $[0 \leq q^2 \leq (m_{B_c} - m_{D_1^0})^2\ \mathrm{GeV}^2]$, and use the total mean lifetime $\tau_{B_c} = (0.46 \pm 0.07)$ ps [21]. Our numerical analysis shows that the contribution of the nonperturbative part (the gluon condensate diagrams) is about 9% of the total and the main contribution comes from the perturbative part of the form factors. Note that, the branching ratios of these decays are very close. This is easily understandable as the only input parameter which differs from the $D_1^0(2420)$ and $D_1^0(2430)$ mesons is their masses (the decay constants are taken to be the same). As far as the $D_1^0(2420)$ meson mass is within the uncertainty interval of the $D_1^0(2430)$ meson mass and the estimate of the branching fractions is practically insensitive to the mass uncertainties, the similarity in the branching fractions is obvious. The value for the branching ratio of this decay is obtained as presented in Table III. The function of the differential decay branching fraction of the $B_c \to D_1^0(2420[2430])l\nu$ ($l = e, \mu$) decays with respect to q^2 is shown in Fig. 6.

The errors are estimated by the variation of the Borel parameters M_1^2 and M_2^2, the variation of the continuum thresholds s_0 and s_0', the leptonic decay constants f_{B_c} and $f_{D_1^0}$, and uncertainties in the values of the other input parameters. The main uncertainty comes from the continuum thresholds and the decay constants, which is about $\sim$25% of the central value, while the other uncertainties are small, constituting a few percent.

It should be noted that the $B_c \to D_1^0 l\nu$ ($l = e, \mu$) decay has been considered for the first time in this paper.

At the end of this section, we would like to compare the value of the branching ratio of this decay with the one of the closely related processes, such as $B_c \to D^* l\nu$ ($l = e, \mu$) decay. The branching fraction predictions for the $B_c \to D^* e\nu$ decay in different approaches are shown in Table IV. The comparison between two processes explicitly indicates the branching ratio suppression of the $B_c \to D_1^0 l\nu$ ($l = e, \mu$) decay.

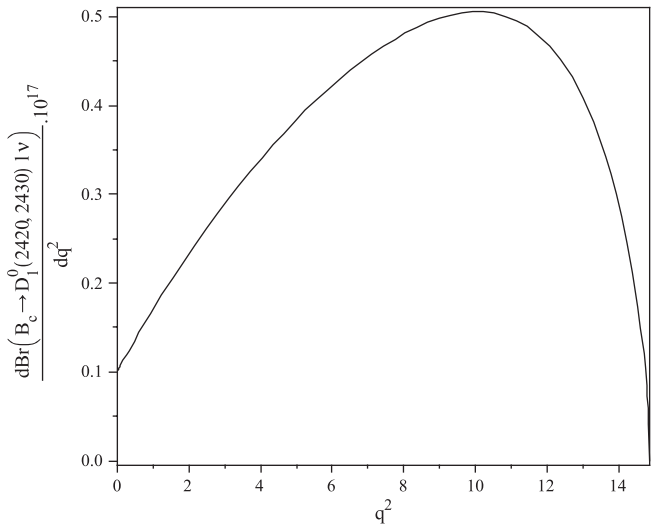

FIG. 6. The dependence of the differential decay branching fraction of the $B_c \to D_1^0(2420[2430])$ decays on q^2.

IV. CONCLUSION

In summary, we analyzed the semileptonic $B_c \to D_1^0(2420[2430])l\nu$ decays in the framework of the three-point QCD sum rules. In this work, the $D_1^0(2420)$ and $D_1^0(2430)$ axial vectors were assumed as conventional $c\bar{u}$ mesons. The related form factors were computed within the 3PSR. The branching ratios of these decays were also estimated. Any future experimental measurement on these form factors as well as decay rates and branching fractions and their comparison with the obtained results in the present work can give considerable information about the structure of these mesons.

ACKNOWLEDGMENTS

We would like to thank K. Azizi for useful discussions.

APPENDIX

In this Appendix, the explicit expressions of the coefficients of the gluon condensate entering the sum rules of the form factors $f_i(q^2)$ ($i = V, 0, 1, 2$) are given.

TABLE IV. The branching ratio of the $B_c \to D^* e\nu$ decay in different approaches: 3PSR with gluon condensate corrections [22], 3PSR without gluon corrections [36], light cone sum rules (LCSR) [37], quark model (QM) [38], and the Bethe-Salpeter equation (BSE) [39].

Mode	3PSR [22]	3PSR [36]	LCSR [37]	QM [38]	BSE [39]
$\mathrm{Br}(B_c \to D^* e\nu) \times 10^{-4}$	(2.2 ± 0.5)	1.8	3.5	3.4	1.8

$$
\begin{aligned}
C_V^4 = {} & -10\hat{I}_1(3,2,2)m_b{}^3m_c{}^2 + 10\hat{I}_1(3,2,2)m_b{}^2m_c{}^3 + 10\hat{I}_2(3,2,2)m_b{}^2m_c{}^3 + 10\hat{I}_0(3,2,2)m_b{}^2m_c{}^3 + 60\hat{I}_2(1,4,1)m_b{}^2m_c \\
& - 20\hat{I}_2(3,2,1)m_b{}^2m_c + 10\hat{I}_2^{[0,1]}(3,2,2)m_b{}^2m_c - 20\hat{I}_0(3,2,1)m_b{}^2m_c + 10\hat{I}_1(3,2,1)m_bm_c{}^2 + 40\hat{I}_2(2,3,1)m_bm_c{}^2 \\
& - 10\hat{I}_0(3,2,1)m_bm_c{}^2 + 20\hat{I}_1(2,3,1)m_bm_c{}^2 - 10\hat{I}_0(3,2,2)m_c{}^5 + 20\hat{I}_1(3,2,1)m_b{}^3 + 10\hat{I}_1(2,2,2)m_b{}^3 \\
& - 20\hat{I}_1(2,3,1)m_b{}^3 + 10\hat{I}_0(3,2,1)m_c{}^3 - 10\hat{I}_2(3,1,2)m_c{}^3 - 20\hat{I}_0(2,2,2)m_c{}^3 - 20\hat{I}_2(2,2,2)m_c{}^3 - 10\hat{I}_0(3,1,2)m_c{}^3 \\
& + 20\hat{I}_0^{[0,1]}(3,2,2)m_c{}^3 - 50\hat{I}_1(2,2,1)m_b + 20\hat{I}_1^{[0,1]}(2,3,1)m_b - 20\hat{I}_1^{[0,1]}(3,1,2)m_b - 20\hat{I}_0(2,2,1)m_b \\
& + 30\hat{I}_1(2,1,2)m_b + 100\hat{I}_2(1,3,1)m_b + 30\hat{I}_0(2,2,1)m_c + 30\hat{I}_2^{[0,1]}(3,1,2)m_c + 20\hat{I}_2^{[0,1]}(3,2,1)m_c \\
& + 10\hat{I}_0^{[0,1]}(3,2,1)m_c + 20\hat{I}_2(2,2,1)m_c - 30\hat{I}_2(2,1,2)m_c + 10\hat{I}_0(3,1,1)m_c + 20\hat{I}_0^{[0,1]}(2,2,2)m_c \\
& + 20\hat{I}_2^{[0,1]}(2,2,2)m_c - 10\hat{I}_2(3,1,1)m_c - 20\hat{I}_1(2,1,2)m_c - 30\hat{I}_0(2,1,2)m_c.
\end{aligned}
$$

$$
\begin{aligned}
C_0^4 = {} & -20\hat{I}_6(3,2,2)m_c{}^5 - 40\hat{I}_6(3,2,1)m_c{}^3 - 20\hat{I}_6(3,1,2)m_c{}^3 + 40\hat{I}_6^{[0,6]}(3,2,2)m_c{}^3 + 20\hat{I}_6(2,2,2)m_b{}^3 + 5\hat{I}_0(2,2,1)m_b{}^3 \\
& - 120\hat{I}_6(1,4,1)m_b{}^3 + 40\hat{I}_6(2,3,1)m_b{}^3 + 10\hat{I}_0^{[0,1]}(2,2,2)m_b{}^3 - 5\hat{I}_0(1,2,2)m_b{}^3 - 20\hat{I}_6^{[0,1]}(3,2,2)m_b{}^3 \\
& + 20\hat{I}_6^{[0,1]}(3,1,2)m_c + 5\hat{I}_0^{[0,1]}(3,1,1)m_c + 5\hat{I}_0(1,1,2)m_c + 20\hat{I}_6(2,1,2)m_c + 40\hat{I}_6(3,1,1)m_c - 10\hat{I}_0^{[0,1]}(1,3,1)m_b \\
& - 15\hat{I}_0(1,2,1)m_b - 40\hat{I}_6(2,2,1)m_b + 15\hat{I}_0^{[0,1]}(2,2,1)m_b - 20\hat{I}_6^{[0,1]}(2,2,2)m_b + 20\hat{I}_6^{[0,2]}(3,2,2)m_b \\
& - 40\hat{I}_6^{[0,1]}(3,1,2)m_b - 15\hat{I}_0(1,1,2)m_b + 10\hat{I}_0^{[0,1]}(3,1,1)m_b - 15\hat{I}_0^{[0,2]}(3,2,1)m_b - 20\hat{I}_6(1,2,2)m_b \\
& - 40\hat{I}_6^{[0,1]}(2,3,1)m_b - 10\hat{I}_0(2,3,1)m_c{}^4m_b + 15\hat{I}_0^{[0,1]}(3,2,2)m_c{}^4m_b + 20\hat{I}_6(3,2,2)m_c{}^4m_b - 15\hat{I}_0(2,2,2)m_c{}^4m_b \\
& + 5\hat{I}_0(3,2,2)m_c{}^5m_b{}^2 - 30\hat{I}_0(1,4,1)m_cm_b{}^4 - 5\hat{I}_0^{[0,1]}(3,2,2)m_cm_b{}^4 + 10\hat{I}_0(3,2,1)m_cm_b{}^4 - 10\hat{I}_0^{[0,1]}(3,2,2)m_c{}^3m_b{}^2 \\
& + 5\hat{I}_0(3,2,1)m_c{}^3m_b{}^2 + 15\hat{I}_0(4,1,1)m_c{}^3m_b{}^2 + 20\hat{I}_6(2,2,2)m_c{}^2m_b + 10\hat{I}_0(1,3,1)m_c{}^2m_b + 20\hat{I}_0^{[0,1]}(3,2,1)m_c{}^2m_b \\
& - 20\hat{I}_0(1,2,2)m_c{}^2m_b - 15\hat{I}_0(2,1,2)m_c{}^2m_b - 10\hat{I}_0(3,1,1)m_c{}^2m_b + 20\hat{I}_6(3,1,2)m_c{}^2m_b + 15\hat{I}_0(2,2,1)m_c{}^2m_b \\
& + 20\hat{I}_0^{[0,1]}(2,3,1)m_c{}^2m_b + 15\hat{I}_0(2,1,2)m_cm_b{}^2 + 5\hat{I}_0(3,1,1)m_cm_b{}^2 - 20\hat{I}_0^{[0,1]}(3,1,2)m_cm_b{}^2 - 20\hat{I}_6(2,2,2)m_cm_b{}^2 \\
& - 10\hat{I}_0(2,2,1)m_cm_b{}^2 + 5\hat{I}_0^{[0,2]}(3,2,2)m_cm_b{}^2.
\end{aligned}
$$

$$
\begin{aligned}
C_1^4 = {} & -40\hat{I}_4^{[0,1]}(2,3,1)m_b + 20\hat{I}_4^{[0,2]}(3,2,2)m_b - 40\hat{I}_3(2,2,1)m_b - 20\hat{I}_1(1,2,2)m_b - 20\hat{I}_3^{[0,1]}(2,2,2)m_b \\
& - 20\hat{I}_3(1,2,2)m_b - 20\hat{I}_4(1,2,2)m_b - 10\hat{I}_1^{[0,1]}(2,3,1)m_b - 15\hat{I}_1(3,2,2){m_c}^5 - 45\hat{I}_1(3,2,1){m_c}^3 - 20\hat{I}_4(3,1,2){m_c}^3 \\
& - 20\hat{I}_2(3,2,1){m_c}^3 - 45\hat{I}_1(4,1,1){m_c}^3 - 20\hat{I}_4(3,2,2){m_c}^5 - 5\hat{I}_0(3,1,2){m_c}^3 - 40\hat{I}_3(2,2,2){m_c}^3 - 15\hat{I}_0(4,1,1){m_c}^3 \\
& - 5\hat{I}_2(3,1,2){m_c}^3 - 10\hat{I}_0(2,2,2){m_c}^3 - 20\hat{I}_1(3,1,2){m_c}^3 - 20\hat{I}_3(3,2,2){m_c}^2{m_b}^3 + 20\hat{I}_4(2,2,2){m_c}^2m_b \\
& - 20\hat{I}_0(2,3,1){m_c}^2m_b + 40\hat{I}_4(3,2,1){m_c}^2m_b + 20\hat{I}_3(3,1,2){m_c}^2m_b + 20\hat{I}_3(2,2,2){m_c}^2m_b + 5\hat{I}_1(3,2,2){m_c}^4m_b \\
& + 20\hat{I}_3(3,2,2){m_c}^4m_b + 15\hat{I}_1(3,2,2){m_c}^3{m_b}^2 + 20\hat{I}_3(3,2,2){m_c}^3{m_b}^2 - 20\hat{I}_4(3,2,2){m_c}^2{m_b}^3 - 5\hat{I}_1(3,2,2){m_c}^2{m_b}^3 \\
& - 50\hat{I}_1(2,3,1){m_c}^2m_b - 10\hat{I}_1^{[0,1]}(3,2,2){m_c}^2m_b + 35\hat{I}_1(3,2,1){m_c}^2m_b + 20\hat{I}_4(3,1,2){m_c}^2m_b + 40\hat{I}_3(2,3,1){m_b}^3 \\
& + 20\hat{I}_3(2,2,2){m_b}^3 - 5\hat{I}_1^{[0,1]}(3,2,2){m_b}^3 + 40\hat{I}_4(2,3,1){m_b}^3 + 20\hat{I}_4(3,2,1){m_b}^3 + 10\hat{I}_1(2,3,1){m_b}^3 \\
& - 30\hat{I}_1(1,4,1){m_b}^3 - 40\hat{I}_4(2,2,2){m_c}^3 - 20\hat{I}_4(2,2,2)m_c{m_b}^2 - 30\hat{I}_1(3,2,1)m_c{m_b}^2 + 90\hat{I}_1(1,4,1)m_c{m_b}^2 \\
& + 120\hat{I}_3(1,4,1)m_3{m_b}^2 + 40\hat{I}_3(3,1,1)m_c - 5\hat{I}_0(2,2,1)m_c + 10\hat{I}_0^{[0,1]}(2,2,2)m_c + 20\hat{I}_4(2,1,2)m_c \\
& + 40\hat{I}_3^{[0,1]}(3,2,1)m_c + 40\hat{I}_4^{[0,1]}(2,2,2)m_c + 5\hat{I}_2(3,1,1)m_c + 20\hat{I}_4(2,2,2){m_b}^3 + 30\hat{I}_0(1,4,1)m_c{m_b}^2 \\
& + 30\hat{I}_2(1,4,1)m_c{m_b}^2 - 20\hat{I}_4(3,2,1)m_c{m_b}^2 + 15\hat{I}_1^{[0,1]}(3,2,2)m_c{m_b}^2 - 10\hat{I}_1(2,2,2)m_c{m_b}^2 - 5\hat{I}_2^{[0,2]}(3,2,2)m_c \\
& + 5\hat{I}_1(2,2,1)m_c + 40\hat{I}_4^{[0,1]}(3,2,1)m_c + 10\hat{I}_2^{[0,1]}(3,2,1)m_c - 5\hat{I}_0^{[0,2]}(3,2,2)m_c + 40\hat{I}_3^{[0,1]}(2,2,2)m_c \\
& + 20\hat{I}_3(2,1,2)m_c - 15\hat{I}_0(2,1,2)m_c + 20\hat{I}_3^{[0,2]}(3,2,2)m_b - 40\hat{I}_3(1,3,1)m_b - 40\hat{I}_4^{[0,1]}(3,1,2)m_b + 10\hat{I}_1(1,3,1)m_b \\
& + 10\hat{I}_0(1,3,1)m_b - 20\hat{I}_4^{[0,1]}(3,2,1)m_b - 20\hat{I}_3^{[0,2]}(3,2,2)m_c - 10\hat{I}_0(3,1,1)m_c.
\end{aligned}
$$

$$
\begin{aligned}
C_2^4 = {} & 15\hat{I}_2(4,1,1){m_c}^2m_b - 40\hat{I}_3^{[0,1]}(3,2,2){m_c}^2m_b - 40\hat{I}_4(3,2,1){m_c}^2m_b - 10\hat{I}_2(2,3,1){m_c}^2m_b + 40\hat{I}_4^{[0,1]}(3,2,2){m_c}^2m_b \\
& - 60\hat{I}_4(4,1,1){m_c}^2m_b + 40\hat{I}_4(2,3,1){m_c}^2m_b + 20\hat{I}_3(2,2,2){m_c}^2m_b - 20\hat{I}_4(3,1,2){m_c}^2m_b + 10\hat{I}_2^{[0,1]}(3,2,2){m_c}^3 \\
& + 60\hat{I}_4(4,1,1){m_c}^3 - 20\hat{I}_3(3,1,2){m_c}^3 - 15\hat{I}_2(4,1,1){m_c}^3 - 5\hat{I}_2(3,2,1){m_c}^3 + 10\hat{I}_1^{[0,1]}(3,2,2){m_c}^3 + 5\hat{I}_0(3,1,2){m_c}^3 \\
& - 5\hat{I}_1(3,1,2){m_c}^3 + 15\hat{I}_0(4,1,1){m_c}^3 - 20\hat{I}_1(3,2,1){m_c}^3 + 20\hat{I}_4^{[0,1]}(3,2,2){m_b}^3 - 20\hat{I}_4^{[0,1]}(3,2,2)m_c{m_b}^2 \\
& + 5\hat{I}_2(3,1,2)m_c{m_b}^2 - 20\hat{I}_3(3,2,1)m_c{m_b}^2 + 20\hat{I}_4(2,2,2)m_c{m_b}^2 - 10\hat{I}_2(2,2,2)m_c{m_b}^2 - 30\hat{I}_0(1,4,1)m_c{m_b}^2 \\
& + 120\hat{I}_3(1,4,1)m_c{m_b}^2 + 5\hat{I}_1^{[0,1]}(3,2,2)m_c{m_b}^2 + 20\hat{I}_4(3,2,1)m_c{m_b}^2 - 10\hat{I}_1(3,2,1)m_c{m_b}^2 + 30\hat{I}_2(1,4,1)m_c{m_b}^2 \\
& + 20\hat{I}_3(2,2,2){m_b}^3 - 20\hat{I}_4(3,2,1){m_b}^3 + 10\hat{I}_2(2,3,1){m_b}^3 + 10\hat{I}_2(3,2,1){m_b}^3 - 120\hat{I}_3(1,4,1){m_b}^3 + 5\hat{I}_0(2,2,1)m_c \\
& + 15\hat{I}_1^{[0,1]}(3,1,2)m_c - 5\hat{I}_2^{[0,2]}(3,2,2)m_c - 15\hat{I}_0^{[0,1]}(3,2,1)m_c + 40\hat{I}_3(3,1,1)m_c + 5\hat{I}_1(3,1,1)m_c \\
& - 20\hat{I}_4^{[0,1]}(3,1,2)m_c + 10\hat{I}_0(3,1,1)m_c + 10\hat{I}_1^{[0,1]}(2,2,2)m_c + 20\hat{I}_3^{[0,1]}(3,1,2)m_c - 20\hat{I}_4(2,1,2)m_c \\
& + 20\hat{I}_3(2,1,2)m_c + 5\hat{I}_2(2,2,1)m_c + 10\hat{I}_2^{[0,1]}(2,2,2)m_c - 15\hat{I}_1(2,1,2)m_c - 15\hat{I}_0^{[0,1]}(3,1,2)m_c - 40\hat{I}_3^{[0,1]}(3,1,2)m_b \\
& + 40\hat{I}_4^{[0,1]}(3,1,2)m_b - 20\hat{I}_2(2,1,2)m_b + 20\hat{I}_4^{[0,1]}(3,2,1)m_b + 5\hat{I}_2^{[0,2]}(3,2,2)m_b + 10\hat{I}_0(2,2,1)m_b - 20\hat{I}_3(2,1,2)m_b \\
& - 10\hat{I}_1(2,2,1)m_b - 20\hat{I}_2(1,2,2)m_b + 20\hat{I}_4(2,1,2)m_b - 40\hat{I}_3(3,1,1)m_b - 10\hat{I}_2(1,3,1)m_b + 20\hat{I}_3^{[0,2]}(3,2,2)m_b \\
& - 40\hat{I}_3(2,2,1)m_b + 20\hat{I}_4^{[0,1]}(2,2,2)m_b + 40\hat{I}_4^{[0,1]}(2,3,1)m_b + 10\hat{I}_2(3,1,2){m_c}^2m_b + 20\hat{I}_4(3,2,2){m_c}^5 \\
& + 5\hat{I}_0(3,2,2){m_c}^5 - 5\hat{I}_2(3,2,2){m_c}^5 + 40\hat{I}_4(3,2,1){m_c}^3 + 40\hat{I}_3^{[0,1]}(3,2,2){m_c}^3 + 20\hat{I}_4(3,1,2){m_c}^3 \\
& + 5\hat{I}_2(3,2,2){m_c}^4m_b + 20\hat{I}_3(3,2,2){m_c}^3{m_b}^2 - 20\hat{I}_4(3,2,2){m_c}^3{m_b}^2 + 5\hat{I}_2(3,2,2){m_c}^3{m_b}^2 - 5\hat{I}_2(3,2,2){m_c}^2{m_b}^3,
\end{aligned}
$$

where

$$
\hat{I}_n^{[i,j]}(a,b,c) = (M_1^2)^i(M_2^2)^j \frac{d^i}{d(M_1^2)^i} \frac{d^j}{d(M_2^2)^j}[(M_1^2)^i(M_2^2)^j\hat{I}_n(a,b,c)].
$$

[1] B. Aubert *et al.* (*BABAR* Collaboration), Phys. Rev. Lett. **90**, 242001 (2003).
[2] D. Besson *et al.* (CLEO Collaboration), Phys. Rev. D **68**, 032002 (2003).
[3] Y. Nikami *et al.* (Belle Collaboration), Phys. Rev. Lett. **92**, 012002 (2004).
[4] P. Krokovny *et al.* (Belle Collaboration), Phys. Rev. Lett. **91**, 262002 (2003).
[5] K. Abe *et al.* (Belle Collaboration), Phys. Rev. D **69**, 112002 (2004).
[6] E. E. Kolomeitsev and M. F. M. Lutz, Phys. Lett. B **582**, 39 (2004).
[7] J. Hofmann and M. F. M. Lutz, Nucl. Phys. **A733**, 142 (2004).
[8] T. Barnes, F. E. Close, and H. J. Lipkin, Phys. Rev. D **68**, 054006 (2003).
[9] H. Y. Cheng and W. S. Hou, Phys. Lett. B **566**, 193 (2003).
[10] H. Kim and Y. Oh, Phys. Rev. D **72**, 074012 (2005).
[11] A. P. Szczepaniak, Phys. Lett. B **567**, 23 (2003).
[12] S. Godfrey and N. Isgur, Phys. Rev. D **32**, 189 (1985).
[13] S. Godfrey, Phys. Rev. D **72**, 054029 (2005).
[14] M. Di Pierro and E. Eichten, Phys. Rev. D **64**, 114004 (2001).
[15] F. E. Close and E. S. Swanson, Phys. Rev. D **72**, 094004 (2005).
[16] E. S. Swanson, Phys. Rep. **429**, 243 (2006).
[17] S. Godfrey, Phys. Lett. B **568**, 254 (2003).
[18] W. A. Bardeen, E. J. Eichten, and C. T. Hill, Phys. Rev. D **68**, 054024 (2003).
[19] M. A. Nowak, M. Rho, and I. Zahed, Acta Phys. Pol. B **35**, 2377 (2004).
[20] J. L. Rosner, Phys. Rev. D **74**, 076006 (2006).
[21] C. Amsler *et al.* (Particle Data Group), Phys. Lett. B **667**, 1 (2008).
[22] N. Ghahramany, R. Khosravi, and K. Azizi, Phys. Rev. D **78**, 116009 (2008).
[23] K. Azizi and R. Khosravi, Phys. Rev. D **78**, 036005 (2008).
[24] E. Eichten and C. Quigg, Phys. Rev. D **49**, 5845 (1994).
[25] S. S. Gershtein *et al.*, Phys. Rev. D **51**, 3613 (1995).
[26] N. Brambilla and A. Vairo, Phys. Rev. D **62**, 094019 (2000).
[27] B. D. Jones and R. M. Woloshyn, Phys. Rev. D **60**, 014502 (1999).
[28] H. P. Shanaham, P. Boyle, C. T. H. Davies, and H. Newton (UKQCD Collaboration), Phys. Lett. B **453**, 289 (1999).
[29] T. M. Aliev and M. Savci, Eur. Phys. J. C **47**, 413 (2006).
[30] V. V. Kiselev, A. K. Likhoded, and A. I. Onishchenko, Nucl. Phys. **B569**, 473 (2000).
[31] B. L. Ioffe and K. N. Zyablyuk, Eur. Phys. J. C **27**, 229 (2003).
[32] P. Colangelo, G. Nardulli, and N. Paver, Z. Phys. C **57**, 43 (1993); V. V. Kiselev and A. V. Tkabladze, Phys. Rev. D **48**, 5208 (1993); T. M. Aliev and O. Yilmaz, Nuovo Cimento Soc. Ital. Fis. A **105**, 827 (1992).
[33] M. A. Shifman, A. I. Vainshtein, and V. I. Zakharov, Nucl. Phys. **B147**, 385 (1979).
[34] P. Colangelo, F. De Fazio, and A. Ozpineci, Phys. Rev. D **72**, 074004 (2005).
[35] T. M. Aliev and M. Savci, Phys. Lett. B **434**, 358 (1998).
[36] V. V. Kiselev, arXiv:hep-ph/0211021.
[37] T. Huang, Z. H. Li, X. G. Wu, and F. Zuo, Int. J. Mod. Phys. A **23**, 3237 (2008).
[38] M. A. Ivanov, J. G. Körner, and P. Santorelli, Phys. Rev. D **63**, 074010 (2001).
[39] C. H. Chang and Y. Q. Chen, Phys. Rev. D **49**, 3399 (1994).